

# Effects of substrate thermal conditions on the swelling of thin intumescent coatings

Andrea Lucherini<sup>1\*</sup>, Jose L. Torero<sup>2</sup>, and Cristian Maluk<sup>1</sup>

<sup>1</sup>School of Civil Engineering, The University of Queensland, Australia

<sup>2</sup>Civil, Environmental & Geomatic Engineering, University College London, UK

## ABSTRACT

The experimental study presented herein investigates the influence of the substrate thermal conditions on the behaviour of thin intumescent coatings. Steel plates coated with a commercially available solvent-based thin intumescent coating were exposed to a constant incident radiant heat flux of 50 kW/m<sup>2</sup> in accordance with the Heat-Transfer Rate Inducing System (H-TRIS) test method. The influence of different substrate thermal conditions was investigated using sample holders capable of controlling the thermal boundary conditions at the unexposed surface of tested steel plates and comparing them to coated timber samples. Experimental results evidence that the substrate thermal conditions govern the swelling of intumescent coatings, thus their effectiveness in protecting load-bearing structural elements. The substrate temperature controls the swelling of intumescent coatings because it defines the temperature experienced by the reacting virgin coating located close to the coating-substrate interface. The physical and thermal properties of the substrate controls the capacity of the system to concentrate/dissipate heat in proximity of the coating-substrate interface. In this way, the substrate thermal conditions governs the temperature evolution of the reacting intumescent coating, consequently the swelling process. Accordingly, high swelling rates were recorded for highly-insulating conditions (timber substrate), while low swelling rates for poorly-insulating conditions (water-cooled heat sink).

## KEYWORDS

Intumescent coatings; substrate thermal conditions; steel structures; swelling; fire testing; H-TRIS; fire safety.

---

\*Corresponding author at: School of Civil Engineering, Advanced Engineering Building (#49), Staff Road House, The University of Queensland, St. Lucia, QLD 4072, Australia.  
Email address: [a.lucherini@uq.edu.au](mailto:a.lucherini@uq.edu.au) (Andrea Lucherini).

## 1 INTRODUCTION AND BACKGROUND

The continuously growing urbanization and world population are pushing for the development of vertical cities. For this purpose, steel represents an optimal construction material due to its ductility, weight-strength ratio, durability and potential for modular constructability<sup>1</sup>. However, the integrity and stability of steel structures can be compromised during and after a fire due to material strength and stiffness losses, as well as thermally-induced forces and displacements<sup>1-2</sup>. The application of different types of thermal barriers is the most common measure to protect steel structures from direct fire exposure. Steel elements are usually covered or wrapped with low conductivity materials to reduce the rate of temperature increase within load-bearing elements<sup>3</sup>. Boards, fire blankets or cement-based spray-on systems are commonly adopted fire safety solutions. However, they are usually deemed to be aesthetically unpleasant and undesirable choice for visible steelwork. For this reason, *intumescent coatings* (also known as reactive coatings) currently represent a worldwide mainstream solution for protecting structural steel systems during fire. Their success is associated with their unique advantages, such as the low impact in the attractive appearance of visible steel structures and their ability to be applied on-site or off-site<sup>4</sup>. Upon sufficient heating, intumescent coatings swell to form a low-density and low-conductivity porous char that prevents the load-bearing steel elements from reaching critical temperatures that can cause structural instability<sup>5</sup>. In the built environment, solvent-based or waterborne thin intumescent coatings are usually applied to a Dry Film Thickness (DFT) no thicker than a few millimetres and, when exposed to heat, they can potentially swell up to 100 times their applied initial DFT<sup>6</sup>. The coating swelling represent a unique peculiarity of intumescent coatings and their insulating effectiveness relies upon the ability of developing a thick, stiff and cohesive porous char.

The majority of the research studies related to intumescent coatings can be generally divided into two main categories. The first category, led by chemists and chemical engineers, focuses on the development and invention of new formulations and ingredients for more effective and reliable intumescent coatings<sup>4,6,7,8</sup>. The second category, led by fire safety engineers, focuses on investigating the overall insulating effectiveness of intumescent coatings as thermal barrier for different structural elements and materials<sup>9</sup>. Based on the research goal, the *swelling of intumescent coatings* is studied and assessed in different manners. Researchers focused on intumescent formulations usually investigate the coating swelling at a small scale. New ingredients and compounds are added and the swelling reaction is analysed in terms of mass loss (Thermo-Gravimetric Analysis, TGA), calorimetry (Differential Scanning Calorimetry,

DSC) or spectroscopy (Fourier-Transform Infrared spectroscopy)<sup>10-13</sup>. On the contrary, within fire safety engineering practice, the insulating performance of intumescent coatings is usually assessed at medium and large scales using furnaces of various sizes<sup>14-19</sup>. These experiments mainly focus on measuring the temperature evolution of coated samples and this parameter is adopted as main performance criteria (i.e. failure is defined as a critical temperature for each specific case). For instance, according to the European method based on the concept of effective thermal conductivity, the complex thermal-physical response of intumescent coatings is simplified in an effective parameter<sup>20-21</sup>. The temperature-dependent effective thermal conductivity defines an equivalent thermal barrier provided by the intumescent coating to the substrate material under a certain heating regime<sup>5,22-24</sup>. This parameter incorporates several phenomena that occur in the intumescent coating, such as the swelling process, endo- and exothermic reactions<sup>9,18</sup>. In this way, the swelling of intumescent coatings is indirectly assessed in terms of a lower temperature rise in the protected material.

In general, the available literature presents limited research studies that have performed detailed analysis of the swelling process of intumescent coatings for real-scale coated samples. Research studies have highlighted the complexities in comprehensively gauging the swelling process of intumescent coatings, both from the physical and thermal aspects<sup>9</sup>. In particular, several challenges are usually experienced in experimentally measuring the actual swelled coating thickness and defining the triggering conditions for the swelling reaction. A recent study investigated how the thermal conditions at the surface of coated steel plates affect the onset of swelling for thin intumescent coatings. Research outcomes defined the temperature ranges for which the swelling reaction was initiated, in terms of temperature experienced by the coating and the steel substrate<sup>25</sup>. However, this research only reported the temperature thresholds for onset of swelling, but the swelling mechanism for medium-scale coated samples was not generally comprehended. In particular, how different thermal conditions at the exposed or unexposed side of the intumescent coating would influence the coating swelling was not fully understood. For example, within the research and regulatory community, ideal adiabatic boundary conditions in all surfaces deemed unexposed usually represent the target conditions, e.g. in standard fire resistance furnace tests<sup>20-21</sup>. Steel elements coated with intumescent coatings are commonly tested in configurations where samples are exposed from all surfaces/sides (e.g. I-profiles) or one-side exposure (e.g. plates). In the two testing configurations, the unexposed surface(s) are usually kept under adiabatic (or close to adiabatic) conditions by placing insulation material in direct contact with the unexposed surface(s) of the

test sample. Since the swelling mechanism is still not fully understood, there is limited understanding on how imposing different thermal conditions at the coating boundaries may influence the swelling process and, in general, the effectiveness of intumescent coatings.

The experimental study presented herein aimed at investigating the influence of the substrate thermal conditions and the effects that this can have on the behaviour of intumescent coatings. Within the scope of this work, steel plates coated with a commercial solvent-based thin intumescent coating were tested using high-performance radiant panels in accordance with the Heat-Transfer Rate Inducing System (H-TRIS) test method<sup>26</sup>. Firstly, the influence of different thermal conditions of steel substrates was investigated using different sample holders that simulate different thermal boundary conditions at the unexposed surface of the test sample. Secondly, the response of the intumescent coating applied on timber substrate and exposed to the same heating conditions was analysed. The described experimental results give a better understanding of the swelling process of intumescent coatings and the influence of the thermal conditions of the steel substrate. In particular, they evidence the direct influence of the substrate temperature on the coating swelling, thus the effectiveness of intumescent coatings. Substrate thermal conditions that do not enable the rise of the substrate temperature can limit the coating swelling and therefore its effectiveness.

## **2 EXPERIMENTAL INVESTIGATION**

### ***2.1 Experimental methodology***

The methodology adopted in this experimental study is based on the Heat-Transfer Rate Inducing System (H-TRIS) proposed by Maluk et al., a well-established test method adopted in research-driven and product development projects for investigating the thermal behaviour of different materials at elevated temperatures<sup>26</sup>. The methodology utilises high-performance radiant panels and it enables the accurate control of the thermal boundary conditions imposed on the test samples with high repeatability and low costs compared with traditional furnace testing. Using a computer-controlled linear motion system, H-TRIS controls the relative position between the target exposed surface of the test sample and an array of radiant panels. In this way, within the limits of minimum and maximum proximities to the exposed surface, test samples can be exposed to any specified time-history of incident radiant heat flux. The experimental setup used within the scope of this work was assembled by combining four high-performance natural-gas-fired radiant heater mounted on a supporting frame, forming a 300 x 400 mm<sup>2</sup> radiant source of heat and able to impose incident radiant heat fluxes up to 100 kW/m<sup>2</sup>

(see Figure 1). Moreover, the experimental methodology enables the visual inspection of the test samples during the thermal exposure (e.g. measuring the swelled coating thickness), technically challenging during conventional standard furnace tests<sup>5,27</sup>.

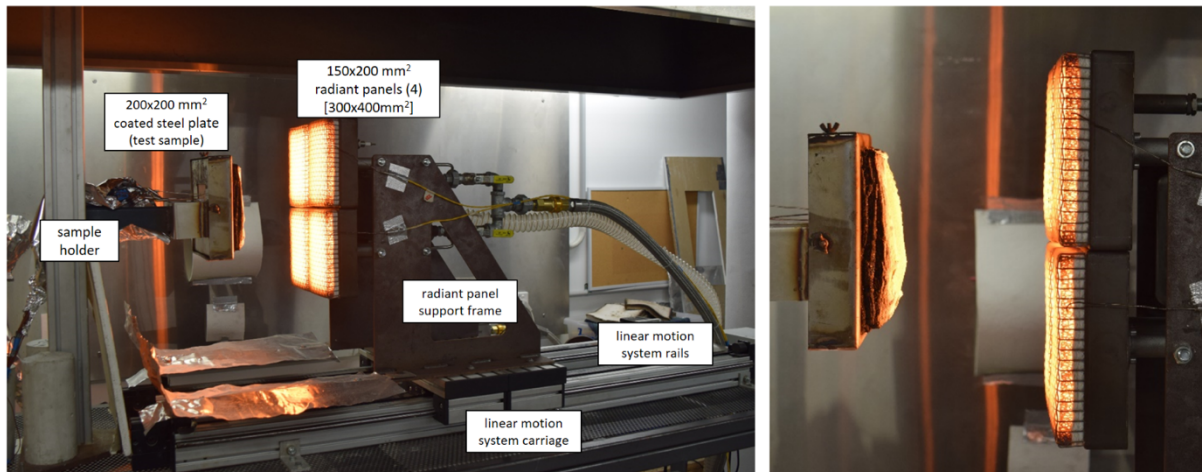


Figure 1. Experimental setup based on H-TRIS test method (*Sample holder A*).

## 2.2 Test samples

The test samples used in this experimental study were 200 x 200 mm<sup>2</sup> mild carbon steel plates with a thickness of 10 mm, resulting in a section factor  $A_p/V$  (i.e. ratio between the exposed surface and volume of steel) equal to 100 m<sup>-1</sup>. Based on the assembled array of radiant panels and a theoretical study on view factors of radiant surfaces, the sample dimensions were chosen in order to achieve a surface distribution of incident radiant heat flux on the sample surface with a deviation lower than 10%. Steel samples were prepared and coated with a thin layer of a commercial solvent-based intumescent coating by a registered professional contractor using airless spray equipment. The product is available in the worldwide market and it is commonly designed for providing up to 120 minutes fire resistance to universal steel sections and cellular beams. It is used for internal, semi-exposed or external applications and it is suitable for off-site and on-site application. The coating was applied in one hand without the use of any primer or topcoat in accordance to the manufacturer guidelines (fast-track coating). After 1 month of curing, the DFT applied on test samples were measured using a non-destructive film thickness gauge at five different locations. The samples were selected in order to have a mean applied DFT in the range 2.10 ± 0.20 mm: the measured values are listed in Table 1.

### 2.3 Experimental setup

The coated steel samples were individually tested using the described H-TRIS test method. Test samples were exposed for 60 minutes to a constant incident radiant heat flux of 50 kW/m<sup>2</sup> at the coated surface. Based on previous research, the heating condition was chosen to ensure a range of temperatures and heating rates higher than the thresholds for onset of swelling of typical thin intumescent coatings<sup>25</sup>. During the thermal exposure, custom-built sample holders were used in order to hold the test sample aligned with the centre-point of the array of radiant panels, in vertical orientation (Figure 1). In particular, two different sample holders were used in order to control the thermal boundary conditions at the unexposed surface of the test sample:

1. *Sample holder A – Adiabatic conditions* (Figure 2a). This setup aims at reproducing adiabatic thermal boundary conditions at the unexposed surface of the test sample. In order to minimise the heat losses, the test sample was insulated at the back using a layer of 20 mm thick ceramic wool (ISOLITE ISOWOOL 1000 BLANKET 100, bulk density 96 kg/m<sup>3</sup>) and 13 mm thick plasterboard (Knauf FireShield). The sample position was secured using a squared stainless steel frame around the sample edges.
2. *Sample holder B – Heat sink conditions* (Figure 2b). A heat sink was in contact with the unexposed surface of the test sample. The heat sink was a 20 mm thick mild carbon steel plate adjacent to a 10 mm thick cavity. This cavity was designed to allow for the circulation of chilled water (about 20°C). The water cavity was included between the heat sink and the 8 mm thick back mild carbon steel plate and contained by a 10 mm steel board frame. Water circulated inside the cavity thanks to a 1/4’’ inlet and 1/4’’ outlet. The water flow into the water cavity was controlled using a volumetric water flow meter. The test sample was secured in place using four steel clamps, two at the bottom and two at the lateral sides of the test sample.

Using the two described sample holders, the experimental investigation was carried out by imposing four different thermal boundary conditions at the unexposed surface of the test sample (refer to Table 1):

1. *Adiabatic conditions (ADC)* – Heat losses at the unexposed surface of the test sample were minimised by using *Sample holder A*.
2. *Heat sink, low rate (HSC1)* – The thermal mass represented by the heat sink was added using the *Sample holder B*. No water circulated inside the cavity.

3. *Heat sink, medium rate* (HSC2) – The heat sink was cooled by a minor water flow, controlled at 0.5 litres per minute (*Sample holder B*).
4. *Heat sink, high rate* (HSC3) – The heat sink was kept cold by a significant continuous water flow, controlled at 10 litres per minute (*Sample holder B*).

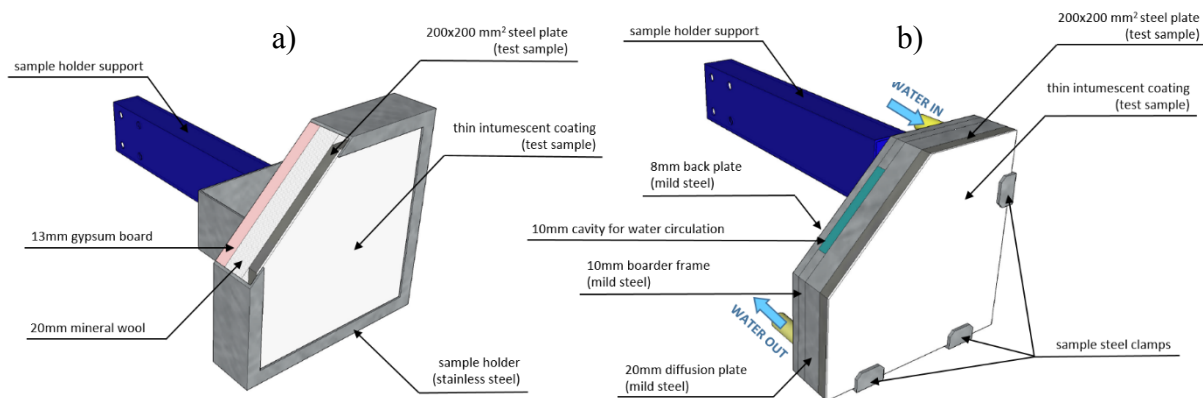


Figure 2. Detailed schematisation of sample holders: a) *Sample holder A* reproducing adiabatic thermal boundary conditions; b) *Sample holder B* reproducing different levels of heat exchange at the unexposed surface of the test sample.

## 2.4 Instrumentation

Up to three K-type thermocouples were attached to the unexposed surface of the test samples in order to measure the evolution of the steel temperature during the thermal exposure. In the cases of experiments with the *Sample holder B*, two K-type thermocouples were placed inside the heat sink at mid-depth by drilling 1.5 mm holes from the lateral side. The thickness of the swelling intumescent coating was measured by image processing of video footages taken using a high-resolution video camera placed at the side of the test sample, aligned with the surface of the test sample (Figure 3). The real-time measurement of the swelled coating thickness was also used for continuously adjusting the relative distance between the intumescent coating surface and the array of radiant panels during the heating exposure. This was done to assure that incident radiant heat flux at the exposed surface of test samples was maintained to the specified value during the full duration of the experiments. In addition, the exposed surface temperature of the intumescent coating was measured using an Infra-Red camera (model DLIR SC655: 16-bit 640 x 480 pixel resolution at 50 Hz, spectral range 7.5 – 14  $\mu\text{m}$ , temperature range up to 2000°C) (Figure 3).

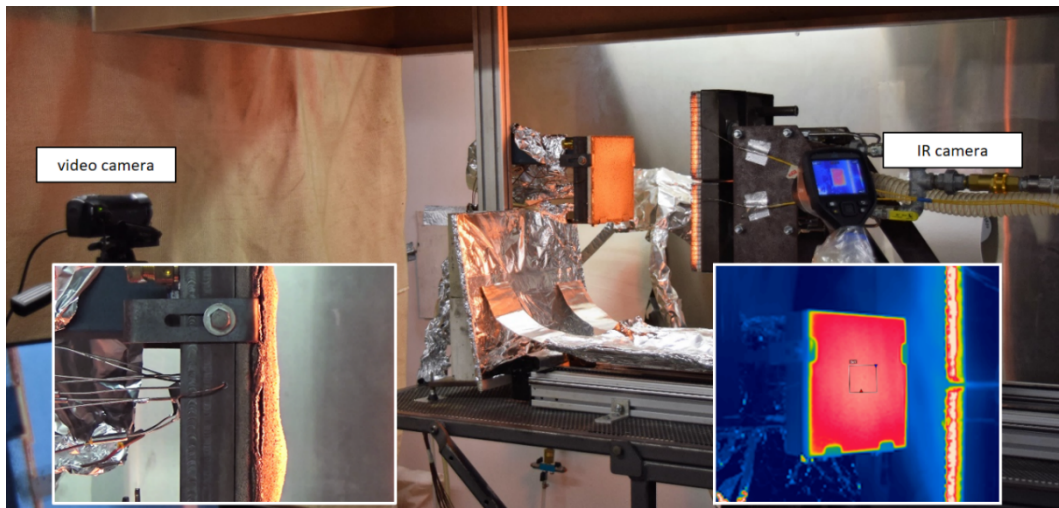


Figure 3. Experimental setup designed to gauge the swelled coating thickness and the surface temperature of intumescent coatings during heating exposure (*Sample holder B*).

### 3 PRELIMINARY INVESTIGATIONS

Before running the main experimental investigation, a few preliminary studies were conducted in order to understand the robustness of the proposed methodology. Following the experimental setup described above, uncoated steel plates were exposed to a constant incident radiant heat flux of  $50 \text{ kW/m}^2$  for 30 minutes. The aim of these studies was to understand if the four different thermal boundary conditions would have exposed the steel to a good variety of temperatures, ranging between two extreme cases: adiabatic conditions and heat sink cooled by a significant continuous water flow. Figure 4 shows the temperature evolution of uncoated steel samples for the four different thermal boundary conditions at the unexposed surface. The four different conditions led to a four distinctive quasi-steady state steel temperatures: about  $640^\circ\text{C}$  for adiabatic conditions and about  $430^\circ\text{C}$ ,  $300^\circ\text{C}$  and  $240^\circ\text{C}$  for conditions involving the heat sink, respectively. This aspect proved the good definition of the different experimental conditions.



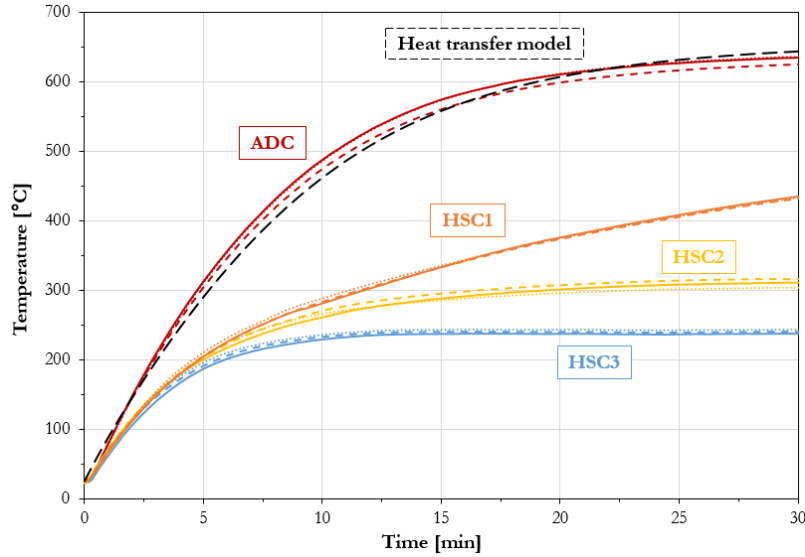


Figure 4. Comparison of the steel temperature evolution for the four different thermal conditions of the steel substrate.

In addition, the experimental results were compared to the solution of a lumped capacitance approximation of transient heat conduction problem for an uncoated steel plate subjected to well-defined thermal boundary conditions<sup>28</sup>. The thermal boundary conditions at the exposed surface were defined by the imposed constant incident radiant heat flux ( $\dot{q}''_{inc}$ ) and the resulting convective ( $\dot{q}''_{conv}$ ) and radiative ( $\dot{q}''_{rad}$ ) heat losses to the surrounding environment. The thermal boundary conditions at the unexposed surface were assumed as ideal adiabatic conditions. General correlations and thermal and physical material properties of carbon steel from the available literature were used<sup>21,25,28</sup>. The good agreement between the heat transfer model and the experimental measurements of the steel substrate temperature supports the assumptions of the thermal conditions at the sample boundaries: adiabatic conditions at the unexposed surface and the specified incident radiant heat flux ( $50 \text{ kW/m}^2$ ) imposed by the H-TRIS test method.

## 4 ANALYSIS AND RESULTS

### 4.1 Visual observations

Thanks to its open environment, the experimental setup based on H-TRIS test method allowed for the visual inspection of the test samples during thermal exposure. As shown in Figure 5, upon heating, the coating underwent different phases, typical of intumescent reactions<sup>9,29</sup>. First, the virgin intumescent coating softens and gradually decompose: this can be observed by the change in colour from white to dark/black and the release of volatiles (“*Thermal decomposition*”).

zone”). After that, the coating gradually swells (“*Swelling zone*”) and forms a carbonaceous porous char (“*Char formation zone*”). Finally, the oxidation reactions occur at the surface of the coating: the intumescent porous char progressively turns into a white/grey colour. In addition, during this final stage, the formation of cracks on the intumescent coating surface is observed: the cracks represent a key vulnerability for the thermal barrier provided by the intumescent coating (“*Char degradation zone*”)<sup>9,29</sup>.

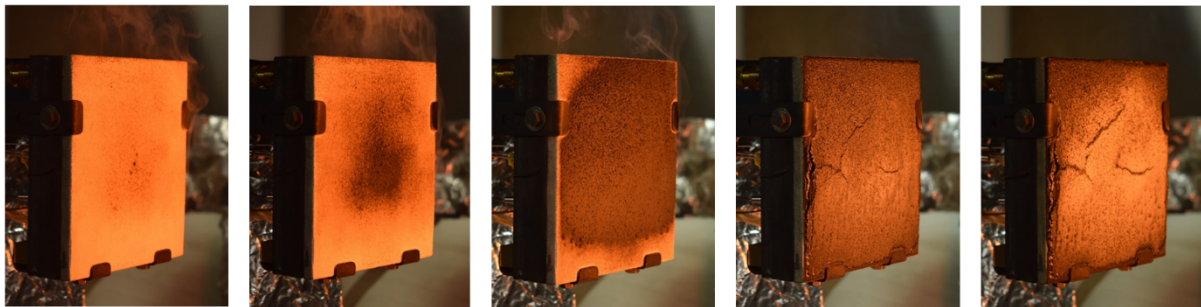


Figure 5. Different phases of the intumescent coating during thermal exposure (sample CP-HSC2-02).

#### 4.2 *Steel temperatures*

The temperature evolution of coated steel samples for the four different thermal boundary conditions was recorded by using thermocouples positioned at the unexposed surface of the test samples. Figure 6 shows the evolution of the steel temperatures for all the experiments carried out on coated samples. The good repeatability between experiments was confirmed by the agreement of the different temperature readings. Throughout all the experiments, the steel temperatures measured using thermocouples has deviations lower than  $\pm 20^{\circ}\text{C}$ . Figure 6 reports the average values of the steel temperatures. In the graphs, the same colour collects all the experiments with the same substrate thermal conditions, while continuous, dashed and dotted lines reports single experimental repetitions.

As predicted in the preliminary investigation on uncoated samples, the four different conditions led to a four distinctive quasi-steady state steel temperatures: about  $340^{\circ}\text{C}$  for adiabatic conditions and about  $250^{\circ}\text{C}$ ,  $150^{\circ}\text{C}$  and  $100^{\circ}\text{C}$  for the experiments involving the heat sink with low (HSC1), medium (HSC2) and high water-cooling rate (HSC3), respectively. This aspect confirmed the good definition of the different experimental conditions aiming at exposing the steel plates to a range of temperatures. However, test samples with different substrate thermal conditions achieved the quasi-steady state steel temperature at different instants during the thermal exposure.

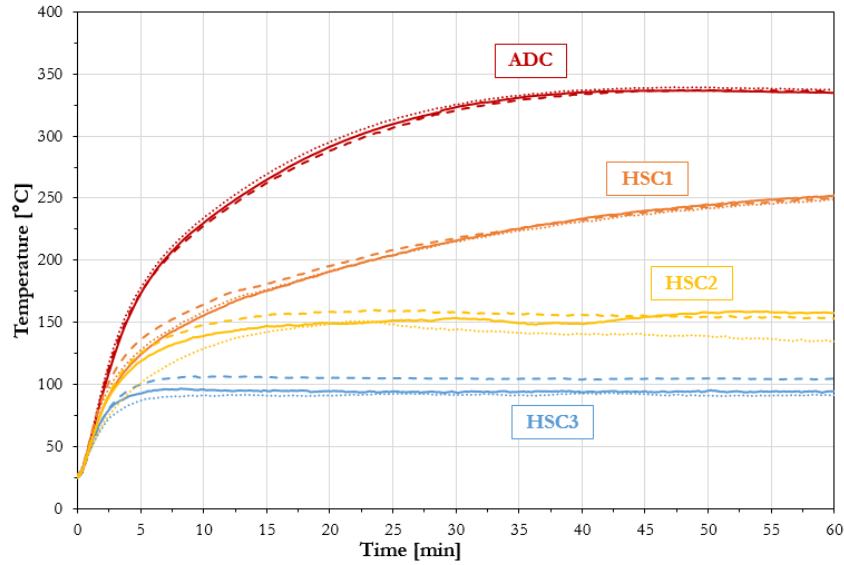


Figure 6. Comparison of the steel temperature evolution for the four different thermal conditions of the steel substrate.

### 4.3 Coating surface temperatures

The temperature evolution at the exposed surface of the intumescent coating was evaluated by post-processing the data obtained using the Infra-Red camera. The coating surface temperature was evaluated by setting a coating emissivity equal to 0.90 and the coating temperature was averaged over a  $50 \times 50 \text{ mm}^2$  area, placed at the centre of the test sample<sup>25</sup>. The emissivity value has a key role in this process and experimental results can be significantly influenced by this parameter. Therefore, a sensitivity analysis of the surface emissivity value of the intumescent coating was performed: the same procedure was repeated for varying coating emissivity  $0.90 \pm 0.02$ , according to the values found in the available literature<sup>18,25,30</sup>. Figure 7 shows the envelope of the temperatures measured at the coating surface in all the experiments carried out on coated samples. During the different experiments, the coating behaved like a low thermal inertia material (thermally thick characterised by a high Biot number) by quickly reaching a certain surface temperature ( $650\text{-}700^\circ\text{C}$ ) and keeping a quasi-constant temperature during the rest of the heating exposure. The substrate thermal conditions did not have a significant effect on the evolution of the coating surface temperature. As expected, the surface temperature of the intumescent coating remained quasi-constant under the same imposed incident heat flux, after an initial transient period (first 5 minutes).

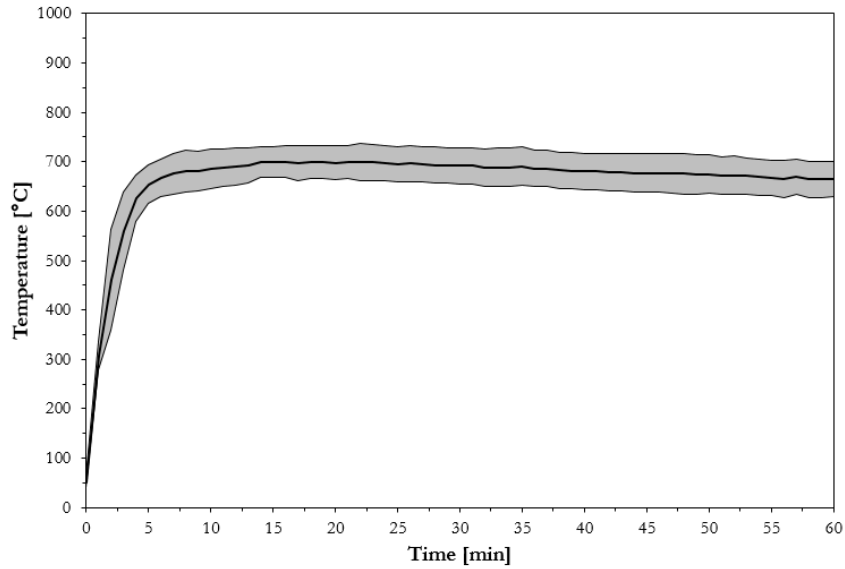


Figure 7. Envelope of the temperature evolution at the coating surface for the four different thermal conditions of the steel substrate.

#### 4.4 Coating swelling

The time-history of coating swelling at the centre of each sample was estimated through image processing of high-resolution video footages. In most experiments, the central area of test samples swelled rather homogeneously and the swelled coating thickness was measured with an accuracy of  $\pm 2$  mm. Figure 8 shows the evolution of the swelled coating thickness for all the experiments carried out on coated samples. Right after the application of the incident radiant heat flux, the intumescent coating started swelling with different rates depending on the substrate thermal conditions, i.e. the slope/derivative of the swelled coating thickness-time curve. In the case of adiabatic conditions at the unexposed surface of test samples, the intumescent coating continuously swelled during the thermal exposure, reaching a maximum thickness of about 50 mm. In the case of different thermal boundary conditions applied using the water-cooled heat sink, the swelling rate decreased for more extreme cooling conditions. In particular, the maximum thicknesses reached at the end of the thermal exposure were about 18 mm, 7 mm or 5 mm for the experiments involving the heat sink with low (HSC1), medium (HSC2) and high water-cooling rate (HSC3), respectively. As a result, the substrate thermal conditions appear to directly govern the swelling of intumescent coatings.

This aspect was also confirmed by the char structures produced by the intumescent coating at the end of the thermal exposure. Figure 9 shows photographs of typical char sections obtained by horizontally slicing the intumescent porous char at mid-height at the end of the thermal exposure. The char structures confirmed that the substrate thermal conditions can significantly

influence the swelling of intumescent coatings. In the case of adiabatic conditions, the intumescent coating swelled homogeneously and created a thick, dense and compact carbonaceous porous media able to effectively protect the substrate material from the thermal exposure. On the other hand, for conditions involving the heat sink, the intumescent coating scarcely swelled and formed a thin carbonaceous layer. In these cases, a large amount of virgin un-reacted coating was observed in the final intumescent char. Figure 10 shows how only the portion of the intumescent coating close to the surface reacted, recognisable by colour changes. On the contrary, the portion of intumescent coating close to the steel did not react due to the significant thermal losses due to conduction through the coating and towards the heat sink. In all experiments, in proximity of the coating surface, it is possible to observe char oxidation: the carbonaceous char turned into ash at the coating crust, characterised by a white-grey colour compared to the dark/black colour of the coating char. Since the surface temperatures exceeded 600°C, oxidation was expected to occur at the coating surface due to the H-TRIS oxygen-rich environment. Based on previous research, it is important to underline that the oxygen content of the exposing atmosphere can have affected the mode and rate of char formation and degradation<sup>31</sup>.

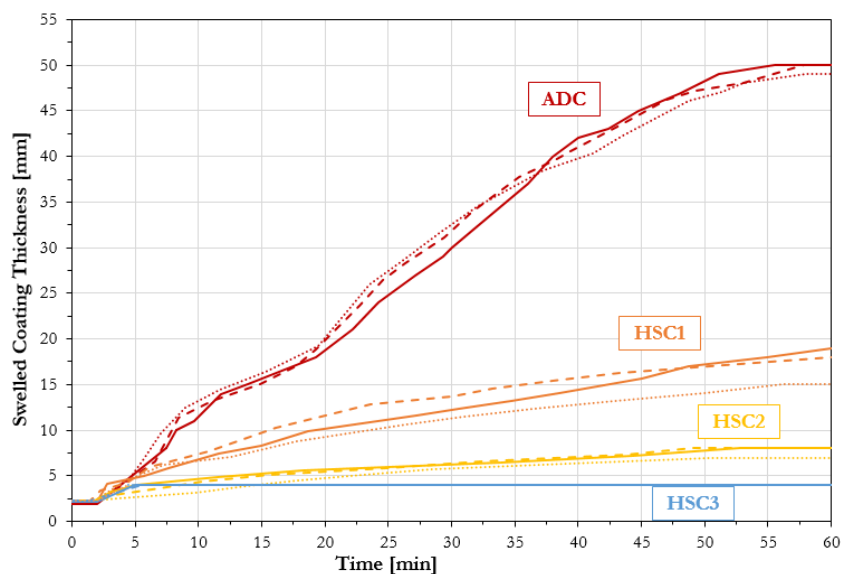


Figure 8. Comparison of the evolution of the swelled coating thickness for the four different thermal conditions of the steel substrate.

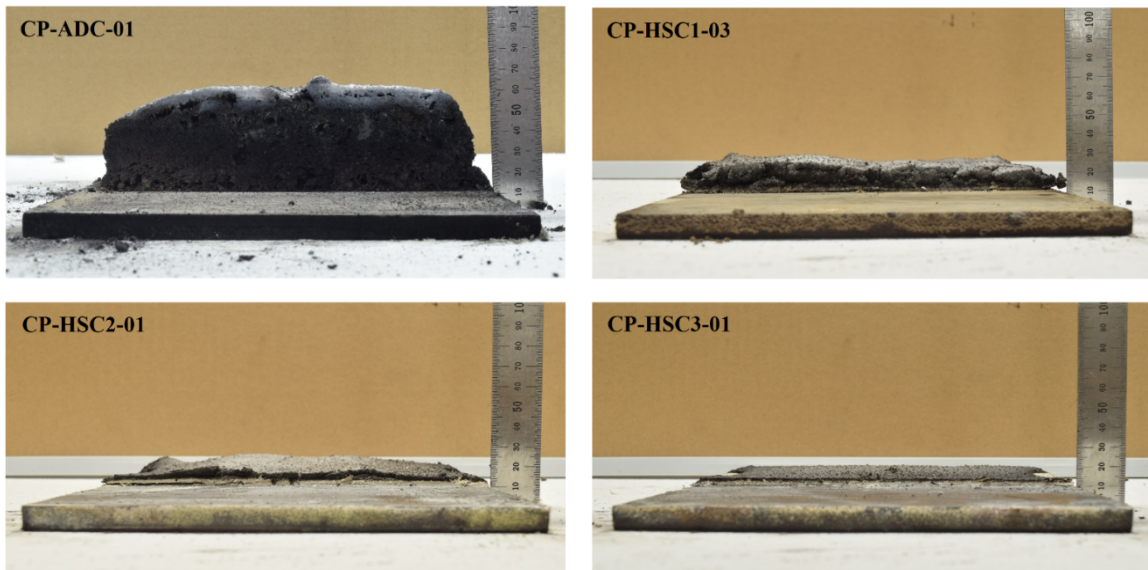


Figure 9. Comparison of typical char sections produced by the intumescent coating at the end of the thermal exposure.



Figure 10. Details of the final intumescent char (sample CP-HSC3-01).

## 5 DISCUSSION

As underlined in the previous paragraphs, the thermal boundary conditions at the unexposed surface of the test sample appear to directly govern the swelling of intumescent coatings. In particular, each thermal condition of the steel substrate can be associated with a certain evolution of the steel substrate temperature and the swelled coating thickness. Figure 11 shows the swelled coating thickness as a function of the steel substrate temperature for the four different experimental setups conducted on coated samples. The plot highlights a direct relationship between the substrate temperature and the swelled coating thickness under the same thermal exposure ( $50 \text{ kW/m}^2$ ). At the same steel temperature, the swelled coating had a very similar thickness for all the different thermal conditions of steel. Particularly, in the experiments involving the water-cooled heat sink, the reduced coating swelling can be related to the low temperature experienced by the steel plates.

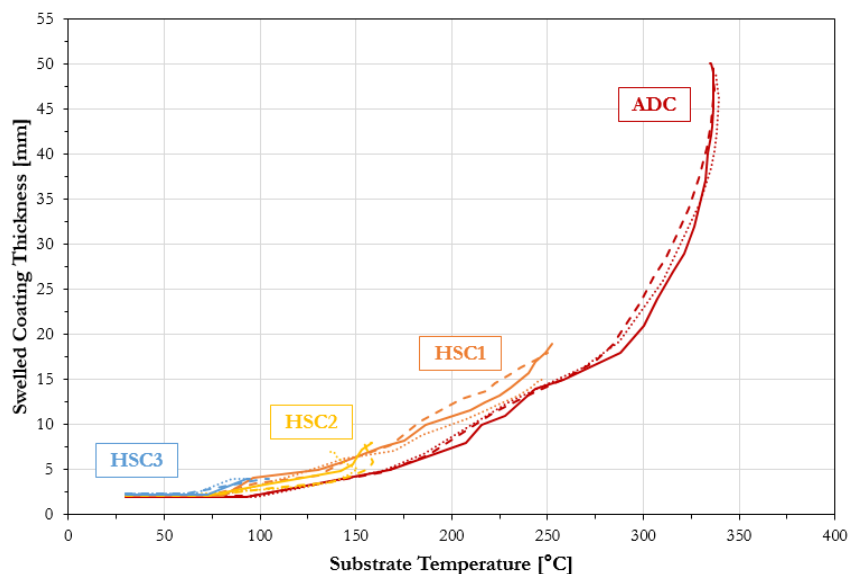


Figure 11. Comparison of the evolution of the swelled coating thickness as a function of the substrate temperature for the four different thermal conditions of the steel substrate.

The described experimental results give a better understanding of the swelling process of intumescent coatings and the influence of the thermal conditions of the steel substrate. Figure 12 shows a simplified schematisation of the thermal conditions of tested samples. Upon heating, the swelled intumescent char, characterised by low thermal conductivity and low density (thermally thick characterised by a high Biot number), quickly reaches a quasi-steady state temperature at the surface ( $T_{surf}$ ) and experiences a steep thermal gradient within its thickness. Within the depth of the intumescent coating, the unreacted virgin coating is located behind the swelled porous char and close to the interface between the steel and the applied coating. At this specific interface, the swelling reaction typically take place. When the virgin coating is above a certain temperature range, the material degrades and chemical reactions occur. In these processes, a large amount of gases are usually produced by the activation of the blowing agent, key compound contained in typical intumescent formulations. The released gases are trapped within the coating thanks to the distinctive physical and mechanical properties (e.g. density and viscosity). The entrapment of gases represent a fundamental process during intumescence in order to optimise the coating swelling. Several researchers have highlighted how the order and the matching of the chemical and physical processes are essential, as they must happen in an appropriate sequence, as the temperature is raised<sup>9,10,25</sup>.

The reacting virgin coating located next to the coating-steel interface is characterised by a low Biot number due to the relatively high thermal conductivity (compared to the swelled intumescent char) and the limited physical thickness. Consequently, the virgin intumescent coating behaves as a thermally thin material and its temperature can be approximated with the

temperature of the steel substrate ( $T_s$ ). Accordingly, the substrate temperature can be directly related to the swelling process because it defines the temperature experienced by the reacting virgin coating, which is located behind the swelled porous char and sustains the swelling process. In particular, the intumescent coating swells and insulates the substrate by displacing the already-swelled coating towards the direction of the heat source. This aspect was also verified by a close investigation of the recorded video footages. As a conclusion, the substrate temperature governs the swelling of intumescent coatings and thermal conditions that do not enable the temperature rise in the substrate material can limit the coating swelling and therefore its effectiveness.

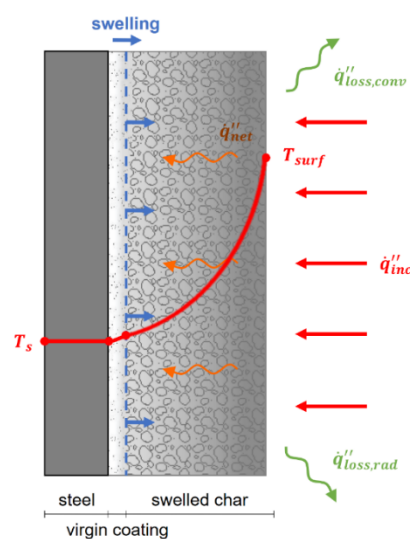


Figure 12. Schematisation of the mechanism of coating swelling.

## 6 APPLICATION TO DIFFERENT SUBSTRATE MATERIAL: TIMBER

The research community is currently looking into the possibility of applying intumescent coatings to protect substrate materials different from steel. For instance, researchers are exploring the advantages of applying intumescent coatings on concrete elements to mitigate the destructive effects of fire-induced spalling and reduce the heat penetration through the concrete into the steel reinforcements<sup>32-33</sup>. In addition, other recent studies have shown that intumescent coatings can be efficiently applied on timber to prevent the occurrence of surface ignition, reduce the flame spread, delay the onset of timber charring and decrease the charring rate within wooden elements<sup>34</sup>. In particular, a research study focused on the application of intumescent coatings on timber elements was recently published<sup>35</sup>. The exploratory investigation adopted the same experimental methodology based on the H-TRIS test method to study the behaviour of coated Cross-Laminated Timber (CLT) blocks subjected to the same heating conditions: a constant incident radiant heat flux of 50 kW/m<sup>2</sup> for 60 minutes. The test



samples had also identical dimensions of the exposed surface, 200 x 200 mm<sup>2</sup>. Test samples were 100 mm thick, composed of 5 lamellae (20mm thick each) of Australian softwood. The tested product was the same commercially available solvent-based thin intumescent coating, applied to a mean Dry Film Thickness (DFT) in a similar range: 2.10 ± 0.20 mm (samples series S21). This research study provides the perfect ground to apply the experimental outcomes presented herein to the case of coated timber samples.

Analogously to this experimental study, the time-history of the coating swelling at the centre of each sample was estimated through image processing of high-resolution video footages. Figure 13 compares the evolution of the swelled coating thickness for all the experiments carried out on coated samples with different substrate thermal conditions, including timber. Contrarily, regarding the evolution of the substrate temperatures, it is difficult to produce a similar plot to the one presented in Figure 6 for the timber case. This is related to the difficulties of estimating the temperature evolution in proximity of the coating-timber interface and the uncertainties related to measuring in-depth temperatures within a low conductivity material like timber<sup>35-36</sup>. Consequently, for the timber case, it is not possible to produce similar plots to the ones shown in Figure 6 and Figure 11. Finally, considering the identical heating conditions, the application of different substrate conditions using timber is expected to have a minor influence on the temperature evolution of the exposed coating surface.

Figure 13 highlights how the timber sample defined another substrate thermal condition for the intumescent coating, fundamentally different to the ones involving steel plates. The comparison of the evolution of the swelled coating thickness confirms that the substrate thermal conditions influence the swelling of intumescent coatings. In the timber case, right after the application of the incident radiant heat flux, the intumescent coating rapidly swelled with a high rate (i.e. slope/derivative of the thickness-time curve), even greater than the one measured for coated steel plates with adiabatic conditions. In addition, the swelling process quickly concluded during the thermal exposure (at about 25 minutes), while in the other cases the intumescent coating continuously swelled during whole duration of the experiment. The main explanation of the different behaviour of the swelling intumescent coating can be directly associated with the thermal conditions produced by the timber substrate. Timber is a low thermal inertia material: when exposed to a heat flux, timber tends to conduct less heat through its thickness and increase its temperature in proximity of its surface. On the contrary, steel is commonly a thermally thin material due to its high thermal conductivity. As a consequence, the temperature evolution at the coating-substrate interface is expected to increase more rapidly than the steel

cases. Following the principles explained in the previous section, the substrate thermal conditions influenced the swelling of the intumescent coating and, in particular, the timber substrate accelerated the swelling process: it created a faster rise of the temperature experienced by the reacting virgin coating, which is located behind the swelled porous char and sustains the swelling process.

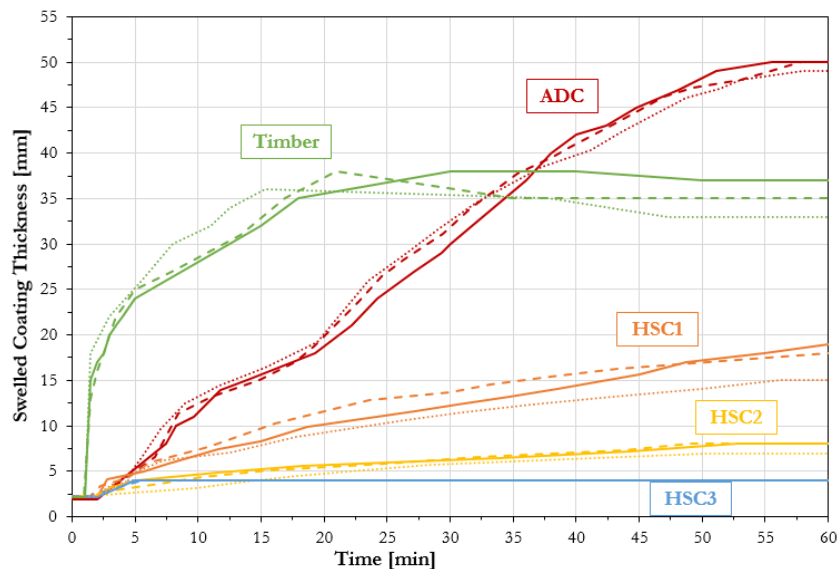


Figure 13. Comparison of the evolution of the swelled coating thickness for the different substrate thermal conditions.

In general, the swelling of intumescent coatings and therefore their effectiveness are governed by the thermal conditions of the substrate and, in particular, by the physical and thermal properties of substrate system. These characteristics control the temperature evolution at the coating-substrate interface, hence the virgin intumescent coating which regulates the swelling reaction. Within the scope of this experimental study, the heating conditions at the exposed surface of the intumescent coating were fixed to a constant incident radiant heat flux of 50 kW/m<sup>2</sup>. From this surface thermal exposure, the tested intumescent coating was expected to receive a similar amount of energy for the different substrate thermal conditions. However, the different substrate thermal conditions controlled the capacity of the system to concentrate and dissipate heat in proximity of the coating-substrate interface. In this way, the substrate thermal conditions controlled the temperature evolution of the reacting intumescent coating and they consequently governed the swelling process. Figure 14 offers a schematic explanation of the different substrate thermal conditions. The use of steel plates, insulated or in contact with the water-cooled heat sink, or timber blocks control the net heat flux into the reacting intumescent coating, defined as control volume within the scope of this experimental study. From the case

that allowed faster coating swelling to the case that essentially prevented coating swelling, the different substrate thermal conditions can be explained as in the following (refer to Figure 14):

- a) *Timber*. The low thermal inertia of timber limits the conduction through its thickness ( $\dot{q}''_{back}$ ) and it enables fast temperature rise in proximity of its surface. Consequently, the intumescent coating quickly reaches onset of swelling and it has a high swelling rate.
- b) *Insulated steel plate*. The steel plate behaves as a thermally thin material due to the high thermal conductivity of steel and the limited physical thickness of the plate. Accordingly, no thermal gradient is expected to develop within the plate thickness. The heat losses at the unexposed surface of the test sample are minimised by the insulation material ( $\dot{q}''_{back}$ ). The steel plate quickly increases its temperature, but it is damped by the relatively high thermal mass of the steel plate ( $\dot{q}''_s$ ), compared to the coating. Consequently, the intumescent coating swells with a lower rate compared to the timber case.
- c) *Steel plate with water-cooled heat sink*. As in the insulated case, the steel plate behaves as a thermally thin material and it increases its temperature according to the thermal mass of the steel plate ( $\dot{q}''_s$ ). However, in this case, significant heat losses are caused by the water-cooled heat sink in contact with the unexposed surface of the test sample ( $\dot{q}''_{back}$ ). The steel temperature rise is directly governed by the heat losses induced by the heat sink. Consequently, the intumescent coating swells with lower rates compared to the insulated steel plate case and the swelling rate decreases with higher cooling due to greater water flows.

Similar concepts could be extended for different substrate materials and steel/timber substrates with different characteristics. For instance, in the case of a thinner steel plate with adiabatic conditions at the unexposed surface, the temperature of the coated steel plate is expected to rise faster than the case of a thicker steel plate due to the lower thermal mass. Consequently, the swelling rate of the intumescent coating is expected to be included between the one measured for the timber substrate (upper bound) and the one measured for the adiabatic conditions of a thicker steel plate (lower bound). Similarly, in the case of a concrete substrate, the swelling rate of the intumescent coating is expected to be slightly lower to the timber case because of the higher thermal inertia of concrete, compared to timber. Nevertheless, it is important to underline that this experimental study did not investigate the potential consequences of adhesion issues between the steel/timber substrate and the tested intumescent coating. The experimental outcomes highlighted within this research assumed good adhesion at the coating-substrate interface. In the case of different materials or intumescent product, particular attention

should be paid for ensuring the good adhesion between the substrate and the protection materials. For instance, in the cited research, the timber charring was avoided by applying a thick intumescent coating (samples series S21) and keeping the temperature within the timber samples below 300°C. Future studies should aim at inspecting this specific aspect.

Unfortunately, within the scope of this experimental study, the substrate thermal conditions can be only explained and analysed in a qualitative manner. The quantification of the thermal conditions obtained involving different substrate systems would be possible only by formulating detailed and complex heat transfer models. However, the problem is characterised by many uncertainties and unknown variables (e.g. thermal and physical properties of the intumescent coating) that make it too complicated and prevent any experimental validation. Overall, future performance-based designs of different systems protected with intumescent coatings should involve the selection of accurate thermal conditions. This experimental study highlighted how the substrate thermal conditions can influence the swelling of intumescent coatings, therefore their effectiveness. At the testing and design stages, the thermal boundary conditions at the exposed and back surfaces of the intumescent coating should be defined with great care. Specifically, the thermal boundary conditions should be as close as possible to the design scenario or they should target the closest critical scenario in order to ensure the safe design of intumescent coatings applied on different substrate materials.

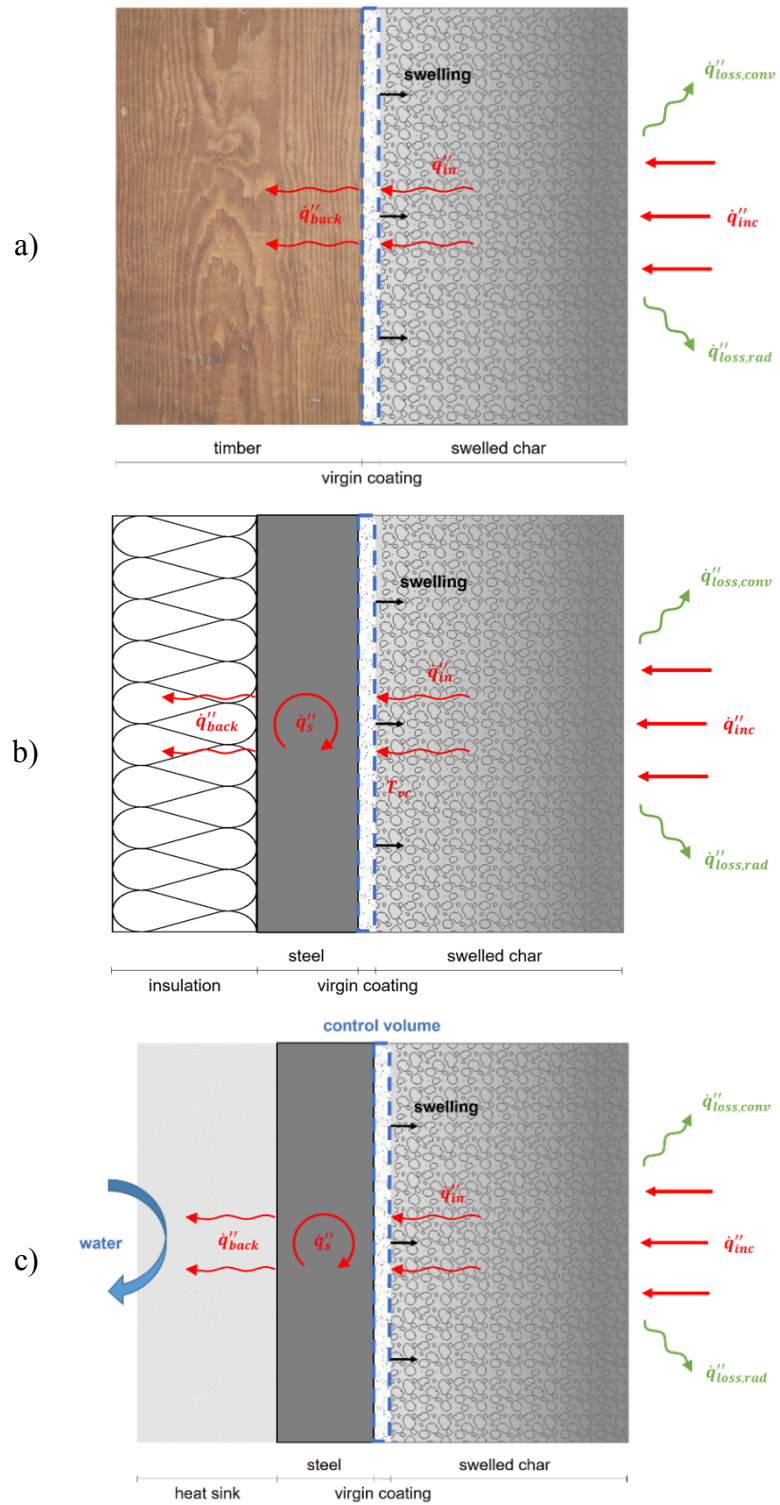


Figure 14. Schematisation of the different substrate thermal conditions.

## 7 CONCLUSIONS

The designed experimental setup and the systematic testing of coated test samples under controlled and highly repeatable heating conditions (at the heated and unheated surface of test samples) enabled the careful investigation of the influence of the substrate thermal conditions and the effects that this can have on the behaviour of thin intumescent coatings.

Within the scope of this work, steel plates coated with a commercial solvent-based thin intumescent coating were exposed to a constant incident radiant heat flux of  $50 \text{ kW/m}^2$  using high-performance radiant panels in accordance with the Heat-Transfer Rate Inducing System (H-TRIS) test method. Firstly, the influence of different thermal conditions of steel substrates was investigated using different sample holders that simulate four different thermal boundary conditions at the unexposed surface of the test sample. Secondly, the response of the intumescent coating applied on timber substrate and exposed to the same heating conditions was analysed.

From the experimental results described herein, the following concluding remarks may be drawn:

- The thermal boundary conditions at the unexposed surface of the test sample directly govern the swelling of intumescent coatings, thus their effectiveness. In particular, under the same thermal exposure ( $50 \text{ kW/m}^2$ ), a direct relationship can be established between the substrate temperature and the swelled coating thickness.
- The described experimental results give a better understanding of the swelling process of intumescent coatings. The swelling reaction takes place at the virgin coating located behind the swelled porous char and close to the interface between the applied coating and the substrate material. The intumescent coating swells and insulates the substrate by displacing the already-swelled coating towards the direction of the heat source.
- The evolution of the substrate temperature governs the swelling of intumescent coatings because it defines the temperature experienced by the reacting virgin coating located close to the coating-substrate interface.
- The physical and thermal conditions of the substrate control the capacity of the system to concentrate and dissipate heat in proximity of the coating-substrate interface. In this way, the substrate thermal conditions govern the temperature evolution of the reacting intumescent coating and consequently the swelling process. Accordingly, the highest swelling rate was recorded for the timber substrate (low thermal inertia), while the lowest

swelling rate was recorded for the water-cooled heat sink with the highest cooling rate (high heat losses).

In general, this experimental investigation highlighted the importance of selecting accurate thermal conditions for the performance-based design of different systems protected with intumescent coatings. The thermal boundary conditions affect the swelling of intumescent coatings and therefore their effectiveness. For example, the current design procedure requires several standard furnace tests on coated steel elements, where some key parameters (e.g. coating initial thickness, section factor and loading) are varied in order to assess the effectiveness of intumescent products in different conditions<sup>20</sup>. As regards the section factor, different section geometries are usually tested within a certain range (e.g. 25-350 m<sup>-1</sup>) and it is accepted to conservatively extend the results to lower or higher values. In the case of heavy steel sections (low section factors), the thermal gradient within the intumescent coating is larger due to the higher thermal mass. According to the experimental outcomes presented herein, the larger thermal gradient may affect the swelling of the intumescent coating, therefore its insulating performance. As a conclusion, the thermal boundary conditions at the exposed and back surfaces of the intumescent coating should be defined and analysed with great care, as close as possible to the design scenario in order to ensure a robust and safe design.

## **ACKNOWLEDGEMENTS**

The authors would like to gratefully acknowledge the support of Qazi Samia Razzaque, Edward Kwok, Long Le and Andrew Abrahams (Remedial Building Services Australia Pty Ltd). The authors are grateful to the Fire Safety Engineering Research Group at The University of Queensland, in particular Dr Juan P. Hidalgo and Mr Jeronimo Carrascal Tirado, for the continuous inspiration, feedback and technical support. The authors would also like to thank the Graduate School of The University of Queensland for financially support Andrea Lucherini with the *2018 Candidate Development Award (CDA)*.

## **CONFLICT OF INTEREST**

The authors declare no conflicts of interest.

## **REFERENCES**

- [1] Wang Y.C. “Steel and composite structures: behaviour and design for fire safety”. Taylor & Francis Group, 2002.

- [2] Usmani A.S., Rotter J.M., Lamont S., Sanad A.M. and Gillie M. “Fundamental principles of structural behaviour under thermal effects”. *Fire Safety Journal*, vol. 36, pp. 721–744, 2001.
- [3] Buchanan A.H. and Abu A.K. “Structural design for fire safety”. John Wiley & Sons, 2nd Edition, 2017.
- [4] Mariappan T. “Recent developments of intumescent fire protection coatings for structural steel: A review”. *Journal of Fire Sciences*, vol. 34, no. 2, pp. 1-44, 2016.
- [5] Elliott A., Temple A., Maluk C. and Bisby L. “Novel testing to study the performance of intumescent coatings under non-standard heating regimes”. *Fire Safety Science – Proceedings of the 11th International Symposium*, University of Canterbury, New Zealand, pp. 652-665, 2014.
- [6] Puri E.G., Khanna A.S. “Intumescent coatings: a review on recent progress”. *Journal of Coatings Technology and Research*, vol. 14, pp.1-20, 2017.
- [7] Weil E.D. “Fire-protective and flame-retardant coatings – A state-of-the-art review”. *Journal of Fire Science*, vol. 29, pp. 259-296, 2011.
- [8] Bourbigot S. and Duquesne S. “Fire retardant polymers: recent developments and opportunities”. *Journal of Material Chemistry*, vol. 17, pp.2283-2300, 2007.
- [9] Lucherini A. and Maluk C. “Intumescent coatings used for the fire-safe design of steel structures: A review”. *Journal of Constructional Steel Research*, vol. 162, n. 105712, 2019.
- [10] Jimenez M., Duquesne S. and Bourbigot S. “Intumescent fire protective coating: toward a better understanding of their mechanism of action”. *Thermochimica Acta*, vol. 449, no. 1-2, pp. 16-26, 2006.
- [11] Bourbigot S. and Duquesne S. “Fire retardant polymers: recent developments and opportunities”. *Journal of Material Chemistry*, vol. 17, pp.2283-2300, 2007.
- [12] Yan L., Xu Z. and Wang X. “Influence of nano-silica on the flame retardancy and smoke suppression properties of transparent intumescent flame-retardant coatings”. *Process in Organic Coatings*, vol. 112, pp. 319-329, 2017.
- [13] de Sa S.C., de Souza M.M., Peres R.S., Zmozinski A.V., Braga R.M., de Araujo Melo D.M. and Ferreira C.A. “Environmentally friendly intumescent coatings formulated with vegetable compounds”. *Process in Organic Coatings*, vol. 113, pp. 47-59, 2017.
- [14] Weisheim W., Schaumann P., Sander L. and Zehfuss J. “Numerical model for the fire protection performance and the design of intumescent coatings on structural steel exposed to natural fires”. *Journal of Structural Fire Engineering*, 2019.



- [15] Wang L., Dong Y., Zhang D., Zhang D. and Zhang C. “Experimental study of heat transfer in intumescent coatings exposed to non-standard furnace curves”. *Fire Technology*, vol. 51, no. 1, pp. 627-643, 2015.
- [16] Zhang Y., Wang Y., Bailey C.G. and Taylor A.P. “Global modelling of fire protection performance of an intumescent coating under different cone calorimeter heating conditions”. *Fire Safety Journal*, vol. 50, pp. 51-62, 2012.
- [17] Li G.Q., Lou G.B., Zhang C., Wang L. and Wang Y. “Assess the fire resistance of intumescent coatings by equivalent constant thermal resistance”. *Fire Technology*, vol. 48, pp. 529-546, 2012.
- [18] Bartholomai M., Schriever R. and Scharrel B. “Influence of external heat flux and coating thickness on the thermal insulation properties of two different intumescent coatings using cone calorimeter and numerical analysis”. *Journal of Fire Materials*, vol. 27, pp. 151-162, 2003.
- [19] Morys M., Illerhaus B., Sturm H. and Scharrel B. “Revealing the inner secrets of intumescence: Advanced standard time temperature oven (STT Mufu+) -  $\mu$ -computed tomography approach”. *Fire and Materials*, vol. 41, pp. 927-939, 2017.
- [20] Comité Européen de Normalization (CEN). “EN 13381-8, Test methods for determining the contribution to the fire resistance of structural members - Part 8: Applied reactive protection to steel members”. Brussel, Belgium, 2013.
- [21] Comité Européen de Normalization (CEN). “EN 1993-1-2:2005 Eurocode 3: Design of steel structures - Part 1-2: General rules - Structural fire design”. Brussels, Belgium, 2005.
- [22] de Silva D., Bilotta A. and Nigro E. “Experimental investigation on steel elements protected with intumescent coating”. *Construction and Building Materials*, vol. 205, pp. 232-244, 2019.
- [23] Cirpici B.K., Wang Y.C. and Rogers B. “Assessment of the thermal conductivity of intumescent coatings in fire”. *Fire Safety Journal*, vol. 81, pp. 74-84, 2016.
- [24] Xu Q., Li G.-Q., Jiang J. and Wang Y.C. “Experimental study of the influence of topcoat on insulation performance of intumescent coatings for steel structures”. *Fire Safety Journal*, vol. 101, pp. 25-38, 2018.
- [25] Lucherini A. and Maluk C. “Assessing the onset of swelling for thin intumescent coatings under a range of heating conditions”. *Fire Safety Journal*, vol. 106, pp. 1-12, 2019.
- [26] Maluk C., Bisby L., Krajcovic M. and Torero J.L. “A Heat-Transfer Inducting System (H-TRIS) test method”. *Fire Safety Journal*, vol. 105, pp. 307-319, 2019.

- [27] Lucherini A. and Maluk C. "Novel test methods for studying the fire performance of thin intumescent coatings". Proceedings of 2nd International Fire Safety Symposium (IFireSS), Napoli, Italy, pp. 565-572, 2017.
- [28] Incropera F.P., DeWitt D.P., Bergman T.L. and Lavine A.S. "Fundamental of heat and mass transfer". John Wiley & Sons, 6th Edition, 2006.
- [29] Lucherini A., Giuliani L. and Jomaas G. "Experimental study of the performance of intumescent coatings exposed to standard and non-standard fire conditions". Fire Safety Journal, vol. 95, pp. 42-50, 2018.
- [30] Omrane A., Wang Y.C., Goransson U., Holmstedt G. and Alden M. "Intumescent coating surface temperature measurement in a cone calorimeter using laser-induced phosphorescence". Fire Safety Journal, vol. 42, pp. 68-74, 2007.
- [31] Griffin G.J., Bicknell A.D. and Brown T.J. "Studies on the effect of atmospheric oxygen content on the thermal resistance of intumescent, fire-retardant coatings". Journal of Fire Sciences, vol. 23, pp. 303-328, 2005.
- [32] Krivenko P.V., Guzii S.G., Bodnarova L., Valek J., Hela R., and Zach J. "Effect of thickness of the intumescent alkali aluminosilicate coating on temperature distribution in reinforced concrete". Journal of Building Engineering, vol. 8, pp. 14-19, 2016.
- [33] Lu F. and Fontana M. "Intumescent coating against explosive spalling of HPC in fire". Proceedings of 5th International Workshop on Concrete Spalling due to Fire Exposure, Borås, Sweden, pp. 365-374, 2017.
- [34] Yan L., Xu Z. and Liu D. "Synthesis and application of novel magnesium phosphate ester flame retardants for transparent intumescent fire-retardant coatings applied on wood substrates". Progress in Organic Coatings, vol. 129, pp. 327-337, 2019.
- [35] Lucherini A., Razzaque Q.S. and Maluk C. "Exploring the fire behaviour of thin intumescent coatings used on timber". Fire Safety Journal, vol. 109, pp. 102887, 2019.
- [36] Beck J.V. "Thermocouple temperature disturbances in low conductivity materials". Journal of Heat Transfer, vol. 84, pp. 124-132, 1962.

Table 1. Experimental matrix.

<b>Sample ID</b>	<b>Substrate thermal conditions</b>	<b>DFT<sub>mean</sub> [mm]</b>
CP-ADC-01	Adiabatic	1.920
CP-ADC-02		2.074
CP-ADC-03		2.014
CP-HSC1-01	Heat sink (low)	2.140
CP-HSC1-02		2.216
CP-HSC1-03		2.226
CP-HSC2-01	Heat sink (medium)	2.230
CP-HSC2-02		2.130
CP-HSC2-03		2.256
CP-HSC3-01	Heat sink (high)	2.162
CP-HSC3-02		2.300
CP-HSC3-03		2.300